

Microstructure and Physical Properties of Hydrogenated 1,4-Poly(2,3-dimethyl-1,3-butadiene)

D. Khlok, Y. Deslandes, and J. Prud'homme*

Department of Chemistry, University of Montreal,
Montreal, Quebec, Canada H3C 3V1. Received April 22, 1976

ABSTRACT: Quantitative hydrogenation of poly(2,3-dimethyl-1,3-butadiene) (PDMB) containing 97% of 1,4-units (74% *trans*, 23% *cis*) has been effected with coordination catalysts derived from triethylaluminum and cobalt(II) 4-cyclohexylbutanoate. Hydrogenated 1,4-PDMB may be considered as either an alternating copolymer of ethylene and 2-butene or a head-to-head:tail-to-tail polypropylene. Proton and carbon-13 NMR spectra of the product suggest that the threo and erythro configurations of the monomer units $-\text{CH}_2-\text{CH}(\text{CH}_3)-\text{CH}(\text{CH}_3)-\text{CH}_2-$ appear with nearly equal frequency in the polymer, indicating that both *cis* and *trans* hydrogenation occurred. X-ray diffraction and DSC measurements indicate that hydrogenated 1,4-PDMB is a completely amorphous elastomeric material with a glass transition temperature 17 K lower than that of atactic head-to-tail polypropylene of the same molecular weight.

In a previous paper¹ we reported the physical and mechanical properties of a polyisoprene hydrogenated SIS block copolymer of styrene and isoprene. Selective and complete hydrogenation of the polyisoprene block was achieved by means of soluble coordination catalyst made by the reaction of triethylaluminum with the cobalt(II) salt of 4-cyclohexylbutanoic acid. The hydrogenation was carried out under low hydrogen pressure and, as shown by both molecular weight and stress-strain measurements, the product did not exhibit any chain degradation. This study on block copolymer was preceded by a more systematic investigation on physical properties of some highly 1,4-homopolydienes hydrogenated by the same technique, including polyisoprene and poly(2,3-dimethyl-1,3-butadiene) (PDMB).

Both polymers were prepared by anionic polymerization using *sec*-butyllithium as initiator and hydrocarbons as solvent. Polyisoprene and PDMB prepared under such conditions contain 93 and 97% of 1,4 units, respectively.^{2,3} The results concerning the first substrate were included in the former report.¹ They confirmed some previous observations^{4,5} that hydrogenated 1,4-polyisoprene is a completely amorphous elastomer with a glass transition temperature only 4 K higher than that of the unhydrogenated material. This compound is of particular interest since hydrogenation of 1,4-polyisoprene leads to an alternating copolymer of ethylene and propylene. In the present paper we describe the results concerning hydrogenated 1,4-PDMB, a compound which may be considered as either an alternating copolymer of ethylene and 2-butene or a head-to-head:tail-to-tail polypropylene. Such alternating structures have already been obtained by copolymerizing directly the olefins with Ziegler–Natta catalysts. For instance, Natta et al.⁶ reported that *cis*-2-butene can be copolymerized with ethylene using $\text{VCl}_4/\text{AlR}_3$ catalysts to lead crystalline alternating copolymers of the erythrodiisotactic type.⁷ Amorphous alternating copolymers of the same olefins were also obtained⁶ by using nonstereospecific catalysts for α -olefins.

Experimental Section

The preparation of the substrate was described elsewhere.³ Its microstructure is 74% *trans*-1,4, 23% *cis*-1,4, and 3% 1,2. Its number average molecular weight determined by osmometry is 4.3×10^4 .

The hydrogenations were carried out on 0.5% polymer solutions in cyclohexane. Catalyst solutions having an aluminum/cobalt molar ratio of 4 were prepared under nitrogen atmosphere by adding slowly a molar solution of triethylaluminum to a 2×10^{-1} M solution of cobalt(II) 4-cyclohexylbutanoate, both in cyclohexane. The catalyst solutions were added to the substrate solutions under nitrogen atmosphere and thereafter hydrogen was bubbled through the solutions at a constant pressure of 4 atm for a period of 2 h, at 50 °C. The molar

percentage of saturated monomer units in the hydrogenated samples was determined by proton NMR spectroscopy.

The proton NMR spectra were measured at 100 °C on a Varian HR-220 spectrometer using chlorobenzene as solvent and tetramethylsilane (TMS) as internal reference. The ¹³C NMR proton noise-decoupled spectra were measured at room temperature on a Bruker WH-90 spectrometer using perdeuteriobenzene as solvent and TMS as internal reference. Approximately 9000 pulses with an acquisition time of 0.7 s were used. Flip angle was 30° and spectral sweep width was 6000 Hz.

The glass transition temperatures were measured on a Perkin-Elmer Model DSC-1B differential scanning calorimeter. The 25-mg samples were run in duplicate at 5, 10, 20, and 40 K/min heating rates. The temperature scale of the instrument was calibrated at each individual heating rate with the melting curves of *n*-dodecane ($T_f = 263.6$ K) and *o*-xylene ($T_f = 248.0$ K).

Results and Discussion

Under the experimental conditions mentioned above, e.g., catalyst having an Al/Co molar ratio of 4 and hydrogen pressure of 4 atm, quantitative hydrogenation of 1,4-PDMB is obtained only for relatively high catalyst concentrations. As shown on Table I, at 5 mol % of catalyst based on PDMB monomer units, only 21% of the unsaturation is hydrogenated. Under similar conditions 100% conversions have been obtained for both 1,4-polyisoprene and SIS block copolymers.¹ A larger hydrogenation time up to 24 h failed to improve the degree of conversion of PDMB at this catalyst concentration. Such a behavior was also observed by Falk⁸ for similar catalyst systems which showed a leveling off of the conversion curve after less than 1 h of reaction. Nevertheless, as shown in Table I, quantitative hydrogenation of PDMB can be achieved by increasing the catalyst concentration up to 30 mol %. The fact that more drastic conditions are required in order to hydrogenate quantitatively 1,4-PDMB is consistent with previous findings⁹ that symmetrically disubstituted olefins are more resistant to catalytic hydrogenation than monosubstituted substrates. On the other hand, number average molecular weight measurements made on two hydrogenated samples (Table I) show that the increase in catalyst concentration did not produce any detectable chain degradation in the material.

Microstructure of Hydrogenated 1,4-PDMB. Figure 1 shows the proton NMR spectrum of completely hydrogenated PDMB observed at 220 MHz in chlorobenzene. Interestingly, the methyl group resonance appears as two doublets near 0.9 ppm indicating that two different configurations can be distinguished for this polymer. As shown on Figure 2 for hydrogenated 1,4-polyisoprene, the expected resonance for a methyl group on a tertiary carbon in a hydrocarbon polymer is a doublet with a coupling constant J of 6.5 Hz. Consequently,

Table I
Degree of Hydrogenation as a Function of [Co]/
[Monomer Units] Ratio and Number Average Molecular
Weight of the Products

| Sample | [Co]/ [monomer units] | Hydrogena- tion, % | $10^{-4}\overline{M}_n$ |
|------------|--------------------------|-----------------------|-------------------------|
| PDMB-4 | | | 4.3 |
| PDMB-4-H-1 | 0.05 | 21 | |
| PDMB-4-H-2 | 0.10 | 26 | 4.2 |
| PDMB-4-H-3 | 0.20 | 62 | |
| PDMB-4-H-4 | 0.30 | 100 | 4.4 |

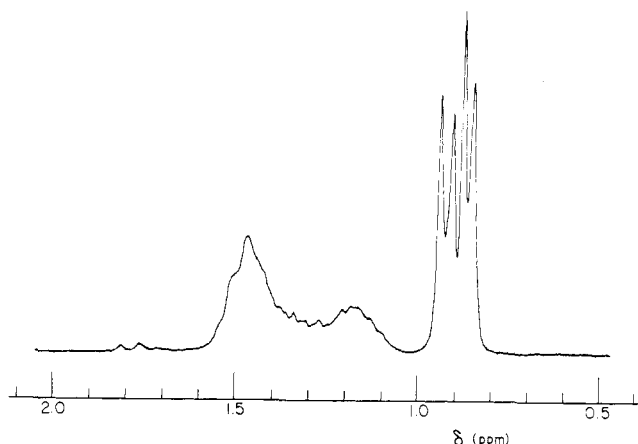
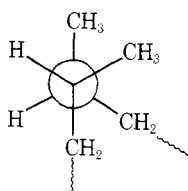
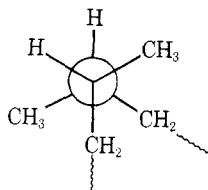


Figure 1. Proton NMR spectrum (220 MHz) of completely hydrogenated 1,4-PDMB. Chlorobenzene solution at 100 °C with tetramethylsilane as reference.

the methyl resonance observed for hydrogenated 1,4-PDMB may be interpreted as the juxtaposition of two doublets with a chemical shift difference of the order of 13.5 Hz. One of these doublets would correspond to the configuration of the erythro type



and the other to the configuration of the threo type



Such a discrimination between erythro and threo configuration is also apparent in the ^{13}C NMR spectrum of hydrogenated PDMB. In fact, as shown in Figure 3, the ^{13}C NMR spectrum of hydrogenated PDMB exhibits six major peaks indicating that two resonances appear for each type of carbon (CH_3 , CH_2 , and CH) present in this polymer. This behavior contrasts with that of hydrogenated 1,4-polyisoprene which shows only four main peaks,^{10,11} one for each type of carbon present in the polymer. The resonances in Figure 3 are numbered 1–6 from high field to low field. Off-resonance decoupling experiments indicated that peaks 1 and 2 correspond to methyl groups, peaks 3 and 4 to methylene groups, and peaks 5 and 6 to methine groups. As mentioned before, the present polymer may be considered as an alternating copolymer of

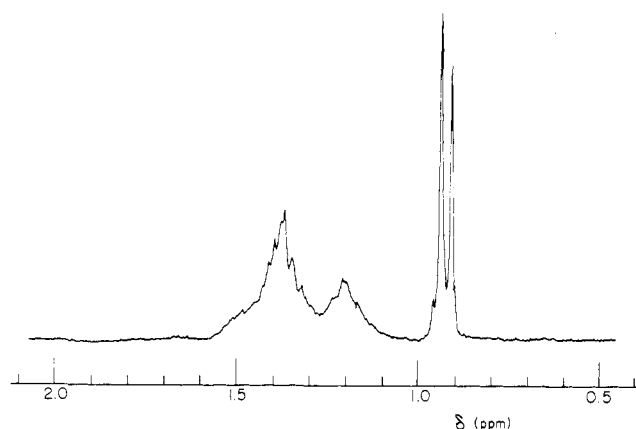


Figure 2. Proton NMR spectrum (220 MHz) of completely hydrogenated 1,4-polyisoprene. Chlorobenzene solution at 100 °C with tetramethylsilane as reference.

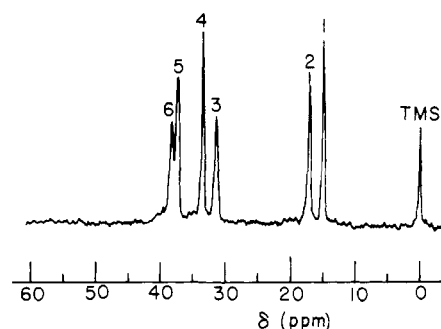


Figure 3. Carbon-13 NMR spectrum (22.63 MHz) of completely hydrogenated 1,4-PDMB. Perdeuteriobenzene solution at room temperature with tetramethylsilane as internal reference.

ethylene and 2-butene. It was thus interesting to compare its carbon resonances with those previously reported by Zambelli et al.¹² for nearly alternating *cis*- and *trans*-2-butene-ethylene copolymers prepared with Ziegler–Natta catalyst. One of these, the *cis*-2-butene copolymer, is a crystalline material. According to Natta et al.,⁷ its structure should be of the erythrodiisotactic type.

Table II contains the chemical shifts of the resonances observed in Figure 3 together with those found by Zambelli et al. for the *cis*- and *trans*-2-butene copolymers. Comparison of the former resonances with those of the *cis*-2-butene copolymer suggests that peaks 2, 3, and 6 in Figure 3 correspond to the erythro structure. An additional methylene resonance at $\delta = 30.3$ ppm was observed by Zambelli et al. for the *cis*-2-butene copolymer. This resonance was attributed to sequences of more than two methylenic groups because the copolymer contained more than 50 mol % of ethylene units.

Turning now to the *trans*-2-butene copolymer studied by Zambelli et al. Table II shows that its methyl and methine resonances coincide perfectly with peaks 1 and 5 in Figure 3, suggesting a threo structure for the butene units of this polymer. However, the main methylene resonance observed for the *trans*-2-butene copolymer does not coincide with the remaining peak 4 in Figure 3. Instead, it appears at 3.0 ppm more upfield. Only a weak but well-resolved resonance can be observed in the spectrum of this polymer at the position of peak 4. The fact that the main methylene resonance was observed at $\delta = 30.5$ ppm, very close to the additional methylene resonance observed for the *cis*-2-butene copolymer and attributed to sequences of more than two methylenic groups, would suggest that the *trans*-2-butene copolymer studied by Zambelli et al. contained considerably more than 50 mol % of ethylene units.

Table II
¹³C Chemical Shifts ^a of Hydrogenated PDMB Compared to Those of *cis*- and *trans*-2-Butene–Ethylene Nearly Alternating Copolymers

| Carbon | Hydrogenated PDMB | Butene–ethylene copolymers ^b | |
|-----------------|-------------------|---|---------------------|
| | | <i>Cis</i> | <i>Trans</i> |
| CH ₃ | 14.7 | | 14.7 |
| CH ₂ | 17.0 | 16.8 | |
| | 31.4 | 30.3 | 30.5 |
| CM | 33.5 | 31.5 | (33.6) ^c |
| | 37.5 | | 37.5 |
| | 38.5 | 38.6 | |

^a All chemical shifts are in ppm downfield from TMS. ^b Data from Zambelli et al.¹² Original chemical shifts were converted using $\delta^{\text{HMDS}} = 2.0$ ppm. ^c Weaker well-resolved peak observed in the Zambelli et al. spectrum.

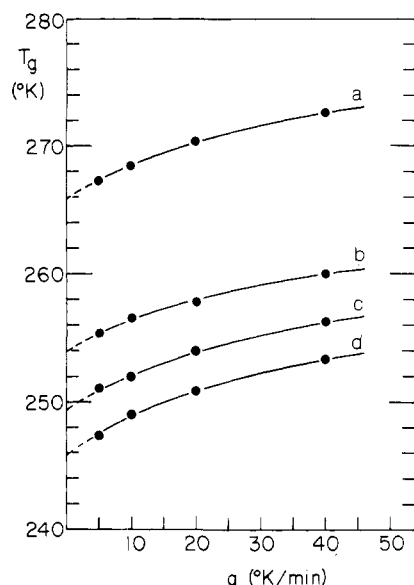


Figure 4. Glass transition temperatures T_g measured by DSC as a function of heating rate q for samples PDMB-4 (a), PDMB-4-H-2 (b), PDMB-4-H-3 (c), and PDMB-4-H-4 (d).

On the basis of the above assignments for the carbon resonances in Figure 3 it is now possible to conclude that the threo structure is predominant in the present hydrogenated PDMB. This is substantiated by the larger intensities of peaks 1, 4, and 5 compared to those of peaks 2, 3, and 6 which were assigned to the erythro structure. Quantitative measurements of the relative intensities of the threo and erythro signals have been made assuming equal Overhauser enhancement for each carbon and assuming negligible spin–lattice relaxation effects. For that purpose the area of each resonance has been measured by cutting and weighing each signal in an expanded scale spectrum. The molar concentration of threo structures measured from the relative area of the methyl signals is 0.54, while the results obtained from the methylene and the methine signals are close to 0.58 and 0.57, respectively. This discrepancy might be explained by various factors including unequal Overhauser enhancements and spin–lattice relaxation effects.

Turning to the proton spectrum of Figure 1, on the basis of the preceding considerations, it is now possible to assign the more shielded methyl doublet to the threo structure. Relative

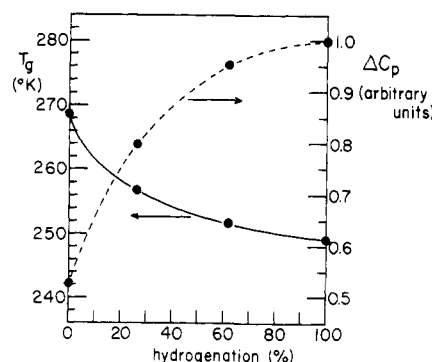


Figure 5. Glass transition temperatures T_g measured at 10 K/min and ΔC_p at T_g measured at 40 K/min as a function of the degree of hydrogenation.

area measurements of the two methyl doublets in this spectrum then lead to a molar concentration close to 0.54 for the threo structure, a result in good agreement with that obtained from the methyl resonances in the carbon NMR spectrum. This result taken in conjunction with the microstructure of the substrate (74% *trans*-1,4 and 23% *cis*-1,4) indicates that both *cis* and *trans* additions occurred during hydrogenation of 1,4-PDMB. A stereospecific *cis* addition, for instance, would have led to 74 mol % of threo structures instead of the observed 54 mol %.

Physical Properties. The x-ray diffraction pattern of completely hydrogenated 1,4-PDMB measured at room temperature consists only of a diffuse halo characteristic of noncrystalline material. This result in conjunction with the glass transition measurements shown below indicates that hydrogenated 1,4-PDMB, like hydrogenated 1,4-polyisoprene, is a completely amorphous elastomeric material at ambient temperature.

Figure 4 shows the glass transition temperature measured on samples described in Table I as a function of heating rate. The samples were previously annealed at 373 K for 15 min and then cooled at a constant rate of 5 K/min to a temperature about 80 K below T_g . The value of T_g was taken as the intersection of the base line below the transition with the extrapolation of the tangent at the point of inflexion in the DSC heating curve. The results show that T_g of completely hydrogenated 1,4-PDMB is 20 K lower than that of the substrate. They also show that this reduction in T_g is not a linear function of the molar percentage of hydrogenated units in the polymer. This behavior is illustrated in Figure 5. It contrasts with that of hydrogenated 1,4-polyisoprene which showed a linear variation of T_g with conversion.¹ The reason for this difference may be in the crystalline nature of 1,4-PDMB prepared with butyllithium in hydrocarbon solvent. In fact, it was previously shown³ that anionic PDMB exhibits an x-ray diffraction pattern identical with that of stereoregular *trans*-1,4-PDMB, indicating the presence of long sequences of *trans* units capable of crystallization in this polymer. Partial hydrogenation even at a low extent, would destroy these sequences and thereby increasing the mobility of the chains would give rise to an abrupt change of T_g at low conversion. Other evidence for that phenomenon is the variation of ΔC_p , the heat capacity increase during glass transition, which, as shown together with T_g in Figure 5, also exhibits an abrupt change at low conversion.

As mentioned before, hydrogenated 1,4-PDMB may be considered as a head-to-head:tail-to-tail polypropylene. From this point of view, it is interesting to note that there is no marked difference between the T_g value measured for this polymer and those quoted in the literature for atactic head-to-tail polypropylene. For instance, using DSC at a heating

rate of 10 K/min, Cowie¹³ found values of T_g close to 266 K for atactic head-to-tail polypropylene fractions of molecular weights in the range 2×10^4 – 6×10^4 . At the same heating rate we measured a T_g close to 249 K for hydrogenated 1,4-PDMP indicating a slightly higher chain mobility for this polymer compared to head-to-tail polypropylene.

Acknowledgments. The authors thank the Canadian 220-MHz NMR Centre for making the proton NMR measurements and Mr. R. Mayer for making the carbon NMR spectra. This work was supported by the National Research Council of Canada and the Quebec Ministry of Education.

References and Notes

- (1) A. Laramée, P. Goursot, and J. Prud'homme, *Makromol. Chem.*, **176**, 3079 (1975).
- (2) J. Prud'homme, J. E. L. Roovers, and S. Bywater, *Eur. Polym. J.*, **8**, 901 (1972).
- (3) D. Blondin, J. Regis, and J. Prud'homme, *Macromolecules*, **7**, 187 (1974).
- (4) G. Gianotti, G. Dall'Asta, A. Valvassori, and V. Zamboni, *Makromol. Chem.*, **149**, 117 (1971).
- (5) L. A. Mango and R. W. Lenz, *Makromol. Chem.*, **163**, 13 (1972).
- (6) G. Natta, G. Dall'Asta, G. Mazzanti, I. Pasquon, A. Valvassori, and A. Zambelli, *J. Am. Chem. Soc.*, **83**, 3343 (1961).
- (7) G. Natta, G. Allegra, I. W. Bassi, P. Corradini, and P. Ganes, *Makromol. Chem.*, **58**, 242 (1962).
- (8) J. C. Falk, *J. Polym. Sci., Part A-1*, **9**, 2617 (1971).
- (9) S. J. Lapporte, *Ann. N.Y. Acad. Sci.*, **158**, 510 (1969).
- (10) C. J. Carman, A. R. Tarpley, and J. H. Goldstein, *Macromolecules*, **6**, 719 (1973).
- (11) Y. Tanaka and K. Hatada, *J. Polym. Sci., Part A-1*, **11**, 2057 (1973).
- (12) A. Zambelli, G. Gatti, S. Sacchi, W. O. Crain, and J. D. Roberts, *Macromolecules*, **4**, 475 (1971).
- (13) J. M. G. Cowie, *Eur. Polym. J.*, **9**, 1041 (1973).

Statistical Mechanical Treatment of Protein Conformation. 4. A Four-State Model for Specific-Sequence Copolymers of Amino Acids¹

Seiji Tanaka^{2a} and Harold A. Scheraga^{*2b}

Department of Chemistry, Cornell University, Ithaca, New York 14853.
Received February 3, 1976

ABSTRACT: One-dimensional short-range interaction models for specific-sequence copolymers of amino acids are being developed in this series of papers. In this paper, our earlier three-state model [involving helical (h), extended (ϵ), and coil (or other) (c) states] is extended to a four-state model by preserving the h and ϵ states, introducing the chain-reversal state (R and S), and redefining the c state. This model involves six parameters ($w_h, v_h, v_\epsilon, v_R, v_S$, and u_c) and requires a 6×6 statistical weight matrix. A nearest-neighbor approximation of the four-state model is also formulated; it requires a 5×5 matrix, involving the same six parameters. By expressing the statistical weights relative to that of the ϵ state, only five parameters ($w_h^*, v_h^*, v_R^*, v_S^*$, and u_c^*) are required in both the 6×6 and 5×5 matrices. The statistical weights for the four-state model are evaluated from the atomic coordinates of the x-ray structures of 26 native proteins. These statistical weights, and the four-state model, are used to develop a procedure to predict the backbone conformations of proteins. Since the prediction of helical and extended conformations is carried out by the procedure described in papers 1–3 of this series, we focus particular attention on chain-reversal conformations in this paper. The conformational-sequence probabilities of finding a residue in h, ϵ , R, S, or c states, and of finding two consecutive residues in a chain-reversal conformation, defined as relative values with respect to their average values over the whole molecule, are calculated for 23 proteins. By comparing these conformational-sequence probabilities to experimental X-ray observations, it was found that, in addition to the prediction of helical and extended conformations (reported in paper 3), 219 chain-reversal regions out of 372 observed by x-ray diffraction studies of 23 proteins were predicted correctly. These results suggest that the assumption of the dominance of short-range interactions in determining chain-reversal (as well as helical or extended) conformations in proteins, on which the predictive scheme is based, is a reasonable one. Finally, in the Appendix, the property of asymmetric nucleation of helical sequences is introduced into the (nearest-neighbor) four-state model.

In this series of papers,^{3–5} we have developed a scheme to predict protein conformations in terms of a one-dimensional model based on short-range interactions. More specifically, we described a method³ for evaluating the statistical weights of conformational states, based on conformational information from x-ray crystal structures of native proteins, and formulated a three-state model⁴ for polypeptide chains, which included α -helical (h), extended (ϵ), and coil (or other) (c) states. This model was used to predict the occurrence of h, ϵ , and c states in proteins.⁵ These will be referred to here as papers 1,³ 2,⁴ and 3,⁵ with equations designated as 1-1, 2-1, etc. In the present paper, we extend the method to a four-state model, consisting of α -helical (h), extended (ϵ), chain-reversal⁶ (R and S), and coil (or other) (c) states. In this extension, we preserve the h and ϵ states of the three-state model,^{3–5} and subdivide the old^{3–5} c state into chain reversals (R and S states, which previously appeared in the c state) and a new (more restricted) c state.

In paper 3,⁵ it was found that a close correlation exists between the regions of high probability of occurrence of h and

ϵ states (calculated with the three-state model) and the helical and extended regions observed experimentally. This attests to the approximate validity of the one-dimensional short-range interaction model for helical and extended conformations in proteins, despite its omission of long-range interactions. Since it was argued previously^{6b,7} that short-range interactions also play a dominant role in determining chain-reversal⁶ conformations, it is of interest to include chain-reversal states in the short-range interaction model. Such chain-reversal conformations are included here in an extension of our earlier three-state model.⁴

In section I of this paper, a theoretical formulation of the four-state model is presented. A nearest-neighbor approximation of the four-state model of section I is discussed in section II. [The property of asymmetric nucleation of helical sequences is incorporated into the four-state model in the Appendix.] In section III, the x-ray data (atomic coordinates) of native proteins are analyzed and, in section IV, these are used to compute the statistical weights of the four-state model. In section V, we consider two procedures for prediction of